

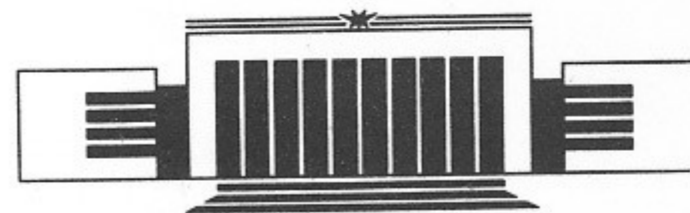


52
ИНСТИТУТ ЯДЕРНОЙ ФИЗИКИ СО АН СССР

V.I. Guselnikov, I.N. Meshkov, T.I. Orishich
V.Ya. Savkin, V.P. Funtikov

ENERGY RECUPERATION
OF INTENSE PROTON BEAM
NEUTRALIZED BY SLOW ELECTRONS

PREPRINT 89-82



НОВОСИБИРСК

Energy Recuperation
of Intense Proton Beam
Neutralized by Slow Electrons

V.I. Guselnikov, I.N. Meshkov, T.I. Orishich
V.Ya. Savkin, V.P. Funtikov

Institute of Nuclear Physics
630090, Novosibirsk 90, USSR

ABSTRACT

Experimental studies of a direct conversion of the energy of intense ion beam are described in the present paper. In the recuperator low electrons are separated with a grid unit, while ions are trapped in one of the three collectors: a flat one, Faraday cup with and without a grid at the input (entrance) window. The efficiency of energy conversion of a proton beam for at a current density up to 150 mA/cm^2 , current pulse duration of $300 \mu\text{s}$ and a power of approximately 0.5 kW is 70% , while at a power of 30 kW the efficiency is about 50% .

Energy recuperation of charged particles in a plasma flow will enable a sufficient increase in the reactor efficiency. Here the problem has two aspects. The first and more easy one concerns the energy recuperation of ions in a plasma flow injected to a plasma heating reactor. In this case, the energy spread of ions is usually insignificant. The second one concerns the energy recuperation of particles in a plasma flow that leaves a reactor. The temperature of particles in this flow is comparable with the average kinetic energy of which fact significantly complicates the problem. Some versions of plasma recuperators were suggested and already partially studied experimentally [1—3]. Their essential difference from the electron beam energy recuperators, which have a well-developed technology (see [4] and its list of references) consists in the necessary separation of plasma flow components and spatial separation over energy. But the problem of an efficient energy recuperation of an ion component is simplified since the receiving surface has positive potential, which automatically suppresses the secondary ion-electron emission, while the secondary ion-ion emission, as a rule, is small. In electron recuperators it is the secondary electron emission that mainly contributes to the collector current loss (losses of the current, captured by a collector).

Described in the present paper are experimental studies of the ion energy recuperation in a beam generated by a proton injector «Start» [5] at a current density of $10\text{—}100 \text{ mA/cm}^2$. In a drift chamber the beam is neutralized by low-energy (ionizing) electrons, so that a plasma flow, where the ion energy spread is smaller than

their average kinetic energy, gets into the recuperator. As distinct from previously published papers [1—3], where experiments were carried out with ion beams, which micropervance did not exceed $10^{-1} \mu\text{A}/\text{V}^{3/2}$ and consequently, the relation of the specific transverse beam size to the Debye radius was equal to 0.01—0.1, in our case the relation of the specific beam size to the Debye radius was equal to 1—10, and so the space charge effects were dominant.

1. DESCRIPTION OF THE INSTALLATION

The experimental set-up (Fig. 1) consists of a proton injector, a one-meter-long drift chamber and a recuperator. The parameters of

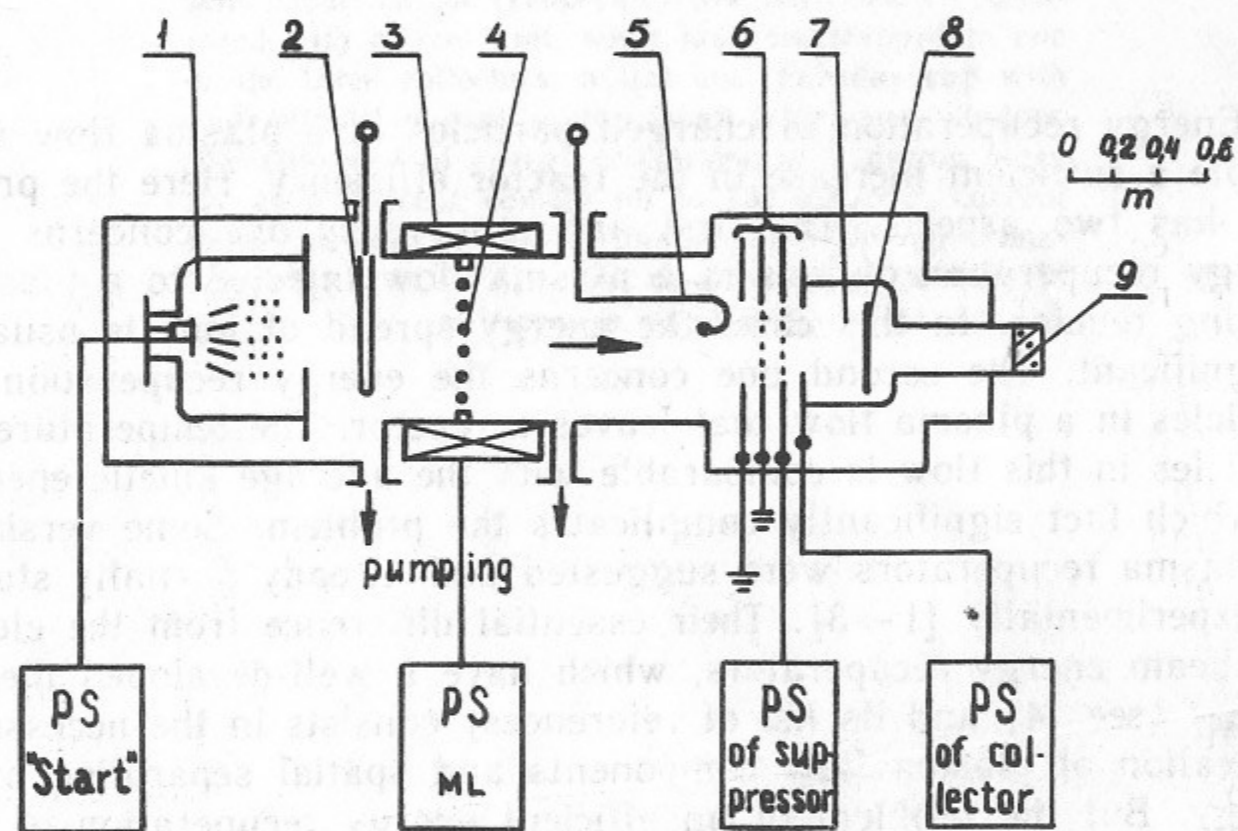


Fig. 1. Schematic lay-out of the experimental set-up:

1—source of proton beam «Start»; 2—aperture diaphragm; 3—magnetic lens; 4—grid for neutralization of a beam space charge; 5—secondary-emission probe; 6—grid unit of the recuperator; 7—collector of the recuperator; 8—foil; 9—observation window; PS—power supply; ML—magnetic lens.

the proton beam injected into the chamber are given in the Table 1. The peculiarity of the «Start»-type injector is the strong dependence (Law 3/2) of the beam current on the accelerating voltage (proton energy). As a result, to reduce the beam current in some experiments there were used aperture diaphragms. The total current of

the beam was controlled by a current transformer (Rogovsky belt) in the injector supply circuit.

Table 1
Proton beam parameters

Proton energy	3—15 keV
Proton current	3—15 A
Beam diameter at the injector output	90 mm
Current pulse duration	200—500 μs
Pulse repetition frequency	0.1 Hz

A cylindrical drift chamber not less than 150 mm in diameter and a volume of about 0.05 m^3 was pumped out by three ion pumps a pumping rate of $1 \text{ m}^3/\text{s}$, the pressure in the chamber was kept at a level of $5 \cdot 10^{-5} \div 5 \cdot 10^{-6}$ Torr (as read the ionization pressure gauge) dependent of the experimental conditions. As a result of the pulsed filling of hydrogen at the moment when the injector came into operation, the pressure increased up to the value of an order of 10^{-4} Torr, then it decreased to the primary value in the course of approximately 3 s.

The beam, which parameters are given in Table 1 has the pervance $10 \mu\text{A}/\text{V}^{3/2}$. Such a beam is «blocked» by its own space charge near the output of the ion source and gets on chamber walls. An ion beam of this intensity can propagate on large distances along the chamber only in case when its space charge is neutralized by low energy electrons knocked out from the chamber walls as a result of a secondary ion-electron emission and electrons born from the ionization of residual gas and hydrogen, out-flowing from the source [6].

To focus the beam into the recuperator a «thick» magnetic lens is placed on the drift section which generates a field up to 0.15 T in its center. Focusing protons, the lens at the same time prevents the low energy electrons born beyond the lens from passing along the beam (magnetic «mirror» effect), and the beam in this is neutralized. To avoid this a grounded grid made of molybdenum wires and having a transparency of 96% is placed inside the lens.

The space distribution of the beam current density was measured in two cross-sections with secondary-emission probes, molybdenum or stainless steel plates 3 mm in diameter: first—be-

hind the focusing lens (at the focusing lens output) and second—before the input aperture diaphragm of the recuperator. A potential of about -40 V was applied to them to reflect low energy electrons accompanying the ion beam.

The position of the beam in the recuperator and the form of its cross-section were registered by a luminescence of a thin ($10 \mu\text{m}$) beam-loaded titanium foil. The beam cross-section had a form of an ellipse with axes ratio 1:1.5.

2. RECUPERATOR. GRID UNIT

In the chosen scheme of the recuperator low energy electrons were separated with a grid unit and ions were gathered in one of the collectors of three types: a flat one, a Faraday cup or a Faraday cup with a grid. Currents at all electrodes of the recuperator were measured with current transformers, calibrated with an accuracy not worse than $\pm 5\%$. The collector and the suppressor grid were supplied from a capacitor bank charged to a required potenti-

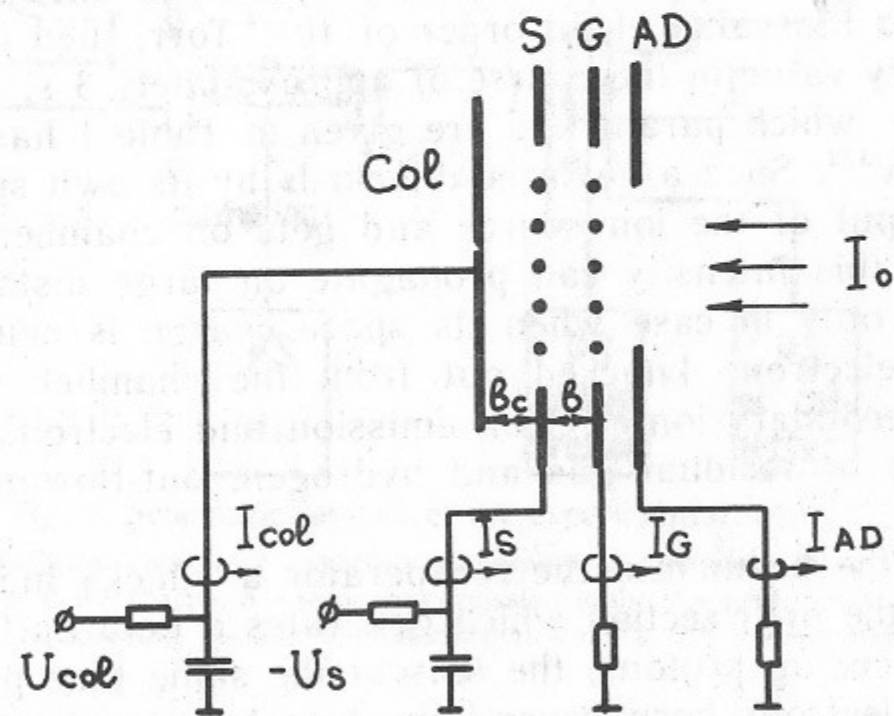


Fig. 2. Scheme of the recuperator with a flat collector and supply circuit of electrodes. $\circ \rightarrow$ —current transformer.

al. The energy reduction on the capacitor bank for a pulse period did not exceed 1%. The grid unit (Fig. 2) consisted of an aperture

diaphragm AD , the first grid G at zero potential, and a suppressor grid S at negative potential U_s . A grounded grid prevents the beam in a drift chamber from being affected by the electric field inside the recuperator. The suppressor grid S serves to repel low energy electrons, which neutralize the space charge of the beam. The aperture diameter AD was specified smaller than the diameter of grid holders to prevent them from incident beam particles. The grids were made of a molybdenum wire 0.2 mm in diameter, baked out in vacuum to reduce its secondary ion-electron emission. The experiments were carried out with two kinds of a grid unit differing in geometric dimensions (Table 2).

Table 2

Geometric Dimensions of Grid Units

Unit	Grid pitch, mm	Grid diameter, mm	Grid diameter, mm	Distance grids, mm	Diameter of opening in diaphragm, mm
Grid unit 1	6	50	60	5	50
Grid unit 2	2	100	100	8	60; 80

The negative potential of the suppressor grid was chosen experimentally and depended on the recuperator geometry and the collector potential. The potential difference $\Delta\varphi$ between the grid cell centre and the grid wire has the order of magnitude

$$\Delta\varphi \sim \left(\frac{U_{col} - U_s}{b_c} - \frac{U_s}{b} \right) h, \quad (1)$$

where U_s , U_{col} are potentials of the suppressor and collector, b , b_c are the distances from the suppressor to the grid G and to the collector, respectively; h is the grid pitch. Electrons with a temperature T_e are repelled by the suppressor, if

$$U_s < U_{scr} \sim - \frac{\frac{T_e}{e} + U_{col} \frac{h}{b_c}}{1 + \frac{h(b_c - b)}{b \cdot b_c}}. \quad (2)$$

For typical values of experimental parameters $\frac{T_e}{e} \ll U_{col} \frac{h}{b_c}$ and $b \sim b_c$, and so formula (2) can be simplified to

$$U_{scr} \sim -U_{col} \frac{h}{b_c}. \quad (3)$$

This formula holds true when $h \leq b_c$.

Presented in Fig. 3 are typical dependences of the collector current on the suppressor grid voltage. Experimentally obtained values of U_{scr} agree with a qualitative dependence (3): U_{scr} increases with the increase of U_{col} and decreases with the decrease of the ratio h/b_c . In the experiments a considerable current was registered on the suppressor grid. For grid unit 1 with a transparency 97% it was $I_s/I_{col} \sim 20-30\%$, while for grid unit 2 with a transparency 90% it was $I_s/I_{col} \sim 60-80\%$.

Taking into account the coefficients of the secondary ion-electron emission γ_{Mo} from the surface of molybdenum wires and of the geometric transparency, one can write

$$\frac{I_s}{I_{col}} = \frac{\chi(1+\gamma_{Mo})}{1-\chi(1+\gamma_{Mo})}, \quad (4)$$

where $\chi = d/h$ — the wire diameter. For molybdenum, at a normal incidence of protons on its surface, at an energy of 10 keV the coefficient of the secondary ion-electron emission is $\gamma_{Mo} \approx 1$ [7, 8]. Then estimations (4) provide the following values:

$$\frac{I_s}{I_{col}} \approx \begin{cases} 6.5\% & \text{for grid unit 1,} \\ 25\% & \text{for grid unit 2.} \end{cases}$$

Thus, the experimental value of the current on the suppressor grid is approximately three times higher than the rated one. This difference is apparently due to the fact that a considerable portion of protons is incident on the cylindrical surface of grid wires at larger angles which causes an increase in the secondary ion-electron emission.

Control experiments with a diagnostics diaphragm placed between the collector and the suppressor spaced about 1 mm from the latter have shown that at $U_{col} < 0.8U_0$ the current on the diaphragm is practically equal to zero. Only when the collector voltage approximates the accelerating one a portion of ions repelled an electric field, hit the diagnostics diaphragm and the suppressor and their current increases.

The high current on the suppressor cannot also be accounted for by the deflection of protons due to the suppressor field. Computer simulation have shown that this effect is negligibly small. The

same conclusion is confirmed by experiments where a dependence of the suppressor grid current was measured at different potentials.

3. RECUPERATOR EFFICIENCY

The efficiency of a recuperator with a double-grid unit (Fig. 3) is described by relation

$$\eta = \frac{U_{col} \cdot I_{col} - U_s \cdot I_s}{U_0 \cdot I_0}, \quad (5)$$

where I_{col} , I_s are currents on the collector and the suppressor respectively, U_{col} , U_s are potentials of the collector and the suppressor,

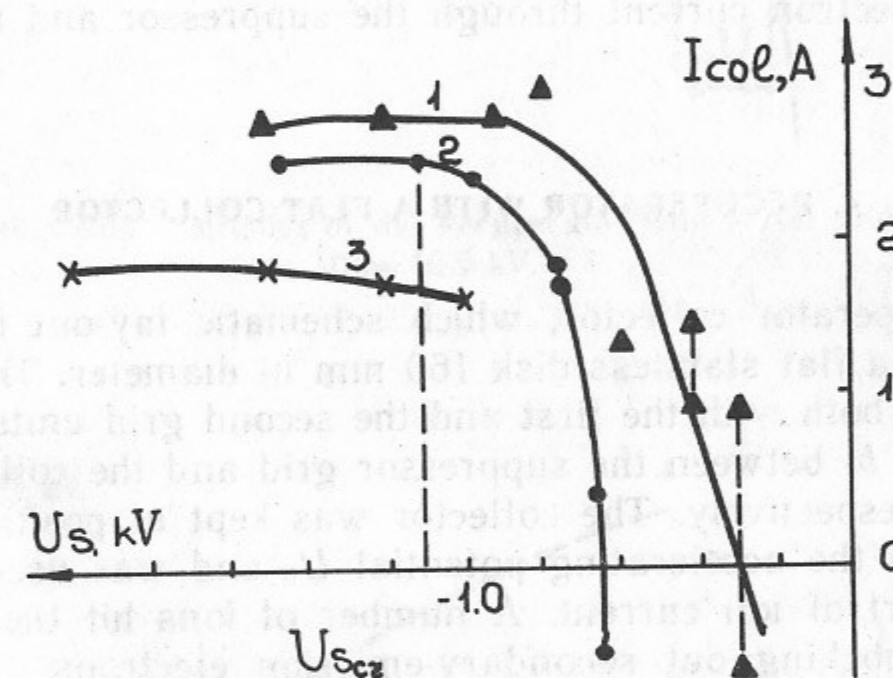


Fig. 3. Dependence of the collector current on the suppressor grid voltage: grid unit 2, $U_0 = 10$ kV:

$U_{col} = 1$ kV (1); $U_{col} = 5$ kV (2); $U_{col} = 8$ kV (3).

U_0 , I_0 is an accelerating voltage of the ion source and the proton current at the entrance into the recuperator. The value of I_0 in this case was taken equal to the sum $I_{col} + I_s$:

$$\eta = \frac{U_{col} \cdot I_{col} - U_s \cdot I_s}{(I_{col} + I_s) U_0}. \quad (6)$$

The secondary ion-electron emission from the suppressor grid reduces considerably the recuperator efficiency, since it results in an

increase in the current on the suppressor and a decrease in the current supplying the collector:

$$I_s = I_s^p + \gamma I_s^p, \quad I_{col} = I_{col}^p - \gamma I_s^p, \quad (7)$$

where γ is the coefficient of the secondary ion-electron emission, I_s^p , I_{col}^p are proton components of the suppressor and the collector currents. Note, that formula (6) gives a correct efficiency value even in the case of the secondary ion-electron emission, if one takes full currents as I_s , I_{col} (7). Then

$$\eta = \frac{I_{col} U_{col} - (U_{col} + U_s) \gamma I_s^p - I_s^p U_s}{(I_{col}^p + I_s^p) U_0}. \quad (8)$$

The second addend in the numerator is the power losses due to the secondary electron current through the suppressor and the collector sources.

4. RECUPERATOR WITH A FLAT COLLECTOR

The recuperator collector, which schematic lay-out is presented in Fig. 2, is a flat stainless disk 160 mm in diameter. The recuperator operated both with the first and the second grid units (Table 2). The distance b_c between the suppressor grid and the collector was 5 and 8 mm respectively. The collector was kept at positive potential U_{col} , close to the accelerating potential U_0 and was used to receive the main part of ion current. A number of ions hit the suppressor grid thus knocking out secondary-emission electrons. The positive current I_0 induced in the circuit of the suppressor grid made up the main part of current losses in the recuperator.

Typical decelerating characteristics, i. e. the dependence of the collector and suppressor currents on the potential of a flat collector is shown in Fig. 4. In point «A» the product of a collector current by its voltage is a maximum. Usually the maximum efficiency of the recuperator is provided in the same point: for example, to characterize Fig. 5 formula (6) gives $\eta = 0.49$. In point «B» the collector current is equal to zero, and the collector potential with an accuracy of the measurements error is equal to the accelerating voltage. The value ΔU , called a «deceleration depth» of a beam is equal to

$$\Delta U = U_{col(B)} - U_{col(A)} \approx U_0 - U_{col(A)}. \quad (9)$$

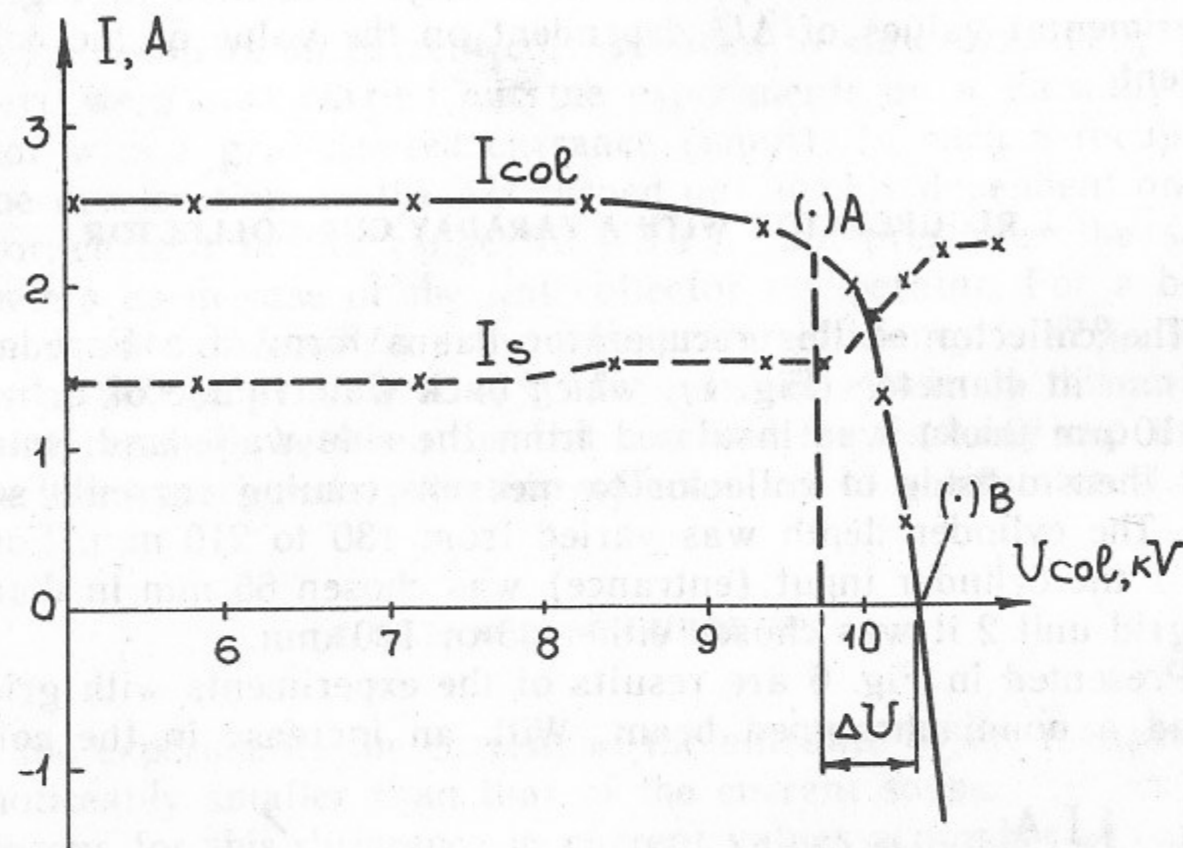


Fig. 4. Deceleration Characteristics of the Recuperator with a flat grid unit collector $U_0 = 10.5$ kV.

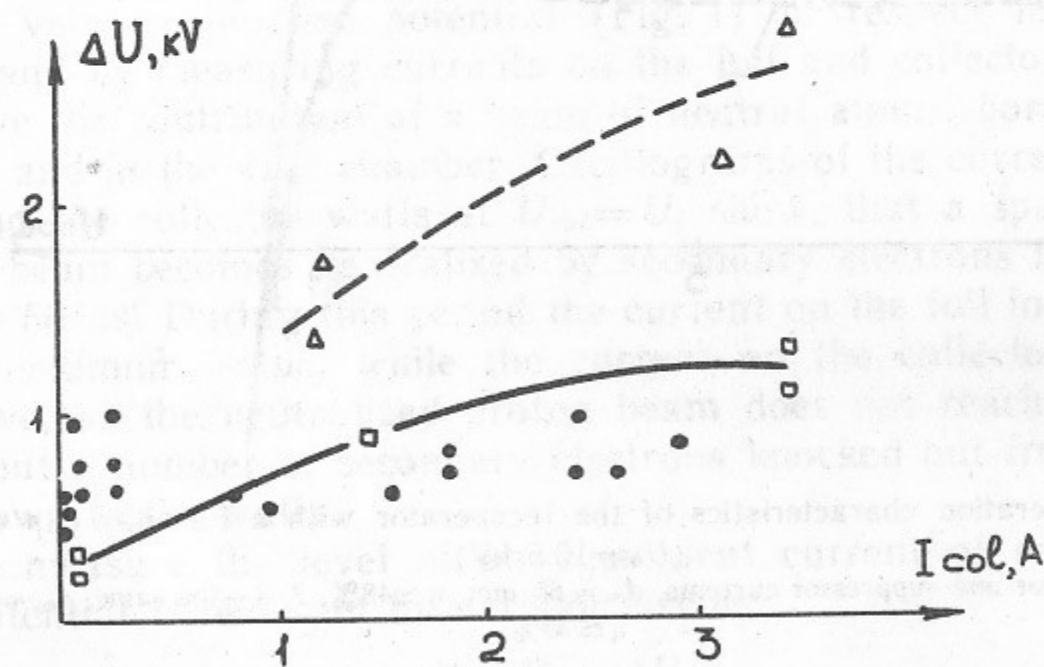


Fig. 5. Dependence of deceleration depth on recuperated current:
● — flat collector; □ — Faraday cup collector, $d_{col} = 65$ mm; △ — the same, $d_{col} = 110$ mm.

It characterizes the recuperator efficiency. Presented in Fig. 5 are experimental values of ΔU dependent on the value of the collector current.

5. RECUPERATOR WITH A FARADAY CUP COLLECTOR

The collector of this recuperator has a form of a Faraday cup 125 mm in diameter (Fig. 1), which back wall (made of a titanium foil 10 μm thick) was insulated from the side walls and connected with them outside of collector to measure coming currents separately. The cylinder depth was varied from 130 to 210 mm. For grid unit 1 the cylinder input (entrance) was chosen 65 mm in diameter, for grid unit 2 it was chosen either 65 or 110 mm.

Presented in Fig. 6 are results of the experiments with grid unit 2 and a nondiaphragmed beam. With an increase in the collector

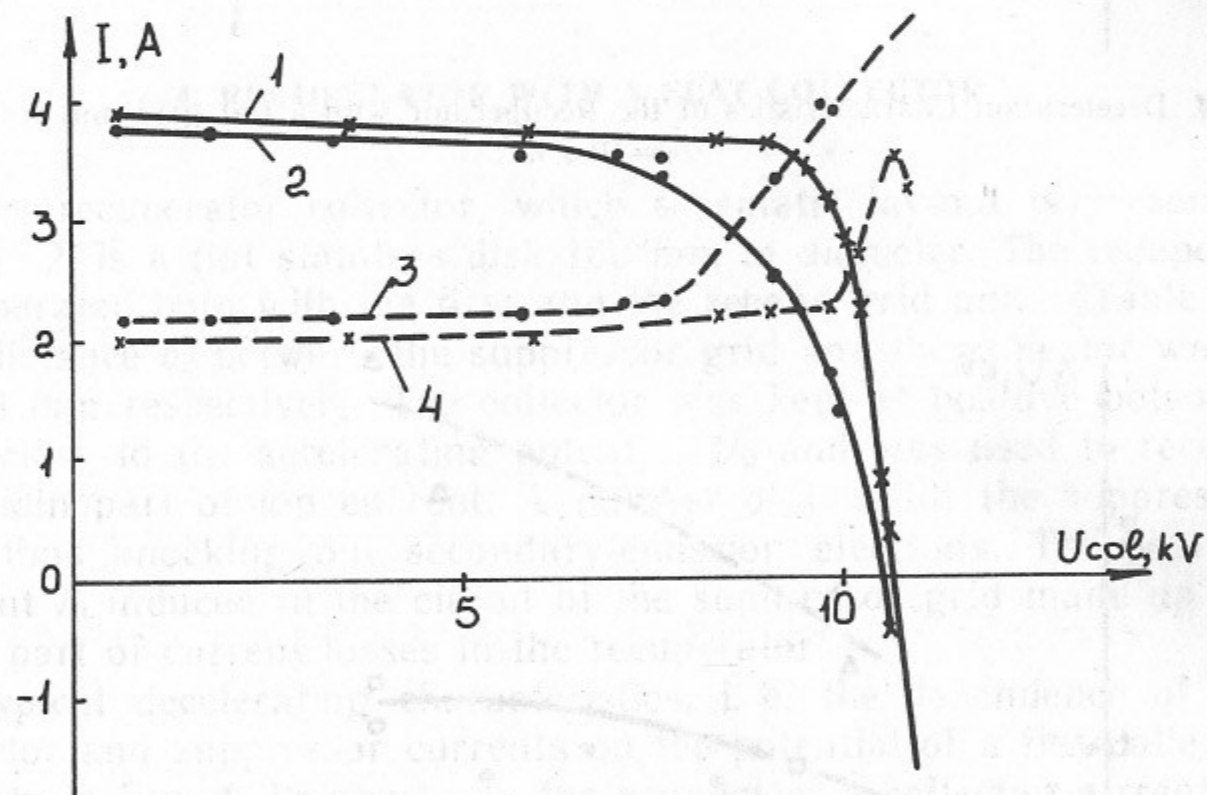


Fig. 6. Deceleration characteristics of the recuperator with a Faraday cup collector ($U_0 = 10.5$ kV):
1, 4 are collector and suppressor currents, $d_{col} = 65$ mm, $\eta \approx 48\%$, 2, 3 — the same, $d_{col} = 110$ mm, $\eta \approx 39\%$.

input diameter from 65 mm up to 110 mm the value of ΔU increased two times, and consequently the efficiency fell from 48 down to 39%. The dependence of a «deceleration depth» on the

value of a recuperated current corresponded to «law 3/2» (Fig. 5).

There were also carried out the experiments on a Faraday cup collector with a grid-covered entrance (input). In such a recuperator «the deceleration depth» ΔU turned out weakly dependent on the collector current in the range 0.1—3.3 A and preserves the same parameters as in case of the flat collector recuperator. For a beam current density of 5 mA/cm² the recuperator efficiency is 67%, for a density of 200 mA/cm² it is 45%. In terms of efficiency this collector is intermediate between the flat one and the Faraday cup therefore further experiments with this collector are of great interest.

6. BALANCE OF CURRENTS

In the experiments the current at the entrance of the recuperator was noticeably smaller than that of the current source. To find out the reasons for this difference in current values a number of experiments was carried out.

An experimental measurement of a current on the additional diaphragm, placed at the collector input (entrance) showed that practically the whole beam entering the recuperator comes to the collector and to the grids of the grid unit.

By varying the foil potential (Fig. 1) in respect to collector walls and by measuring currents on the foil and collector, one can estimate the contribution of a beam of neutral atoms, born near the source and in the drift chamber. Oscillograms of the currents on the foil and the collector walls at $U_{col} = U_f$ show, that a space charge of the beam becomes neutralized by secondary electrons in approximately 50 μs . During this period the current on the foil increases up to its maximum value, while the current on the collector becomes negative, as the neutralized proton beam does not reach the walls now, but a number of secondary electrons knocked out from the foil lick down to the walls.

To measure the level of an equivalent current of neutrals the foil potential U_f was put by varistor circuit:

$$U_f = U_{col} - \delta U,$$

which differed from the collector current by a constant value δU . The dependences of collector and foil currents on the collector potential for $U_f = 1000$ V are given in Fig. 7. In the region of poten-

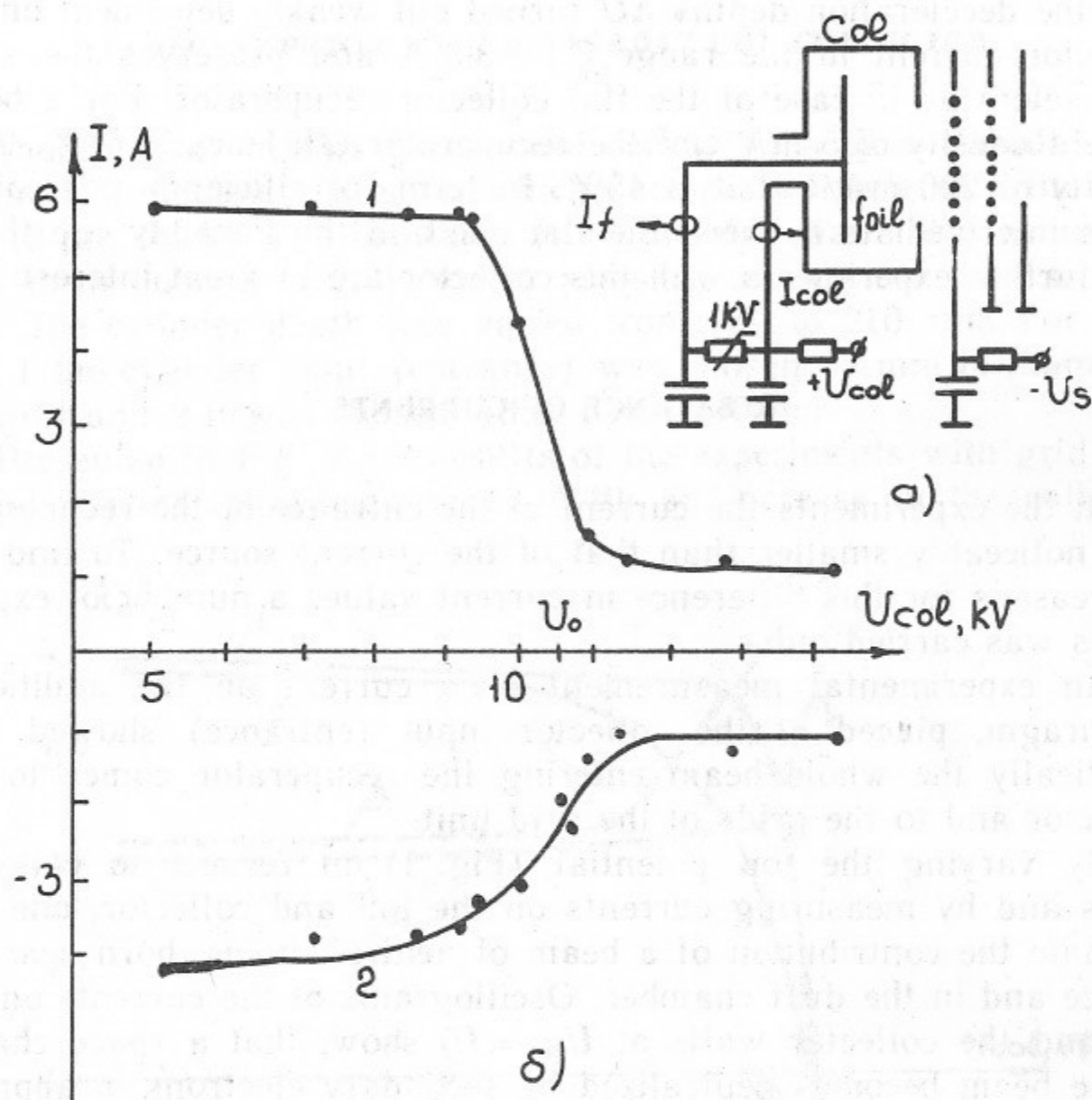


Fig. 7. Schematic lay-out of the experiment on measuring equivalent current of neutrals in the recuperator (a) and deceleration characteristics (b) at $\delta U = 1000$ V:
1 — foil current; 2 — collector current.

tials $I_{col} < U_f$ the total current I_0 in the recuperator consists of a proton current I^p and an equivalent current of neutrals I^n . The electrons knocked out from the surface of the suppressor grid also arrive into the recuperator. The equations of current balance for the regions $U_{col} \ll U_0$ and $U_{col} \gg U_0$ for the known values of coefficients of the secondary electron-electron emission from the titanium surface permit to calculate the value of a coefficient of the secondary ion-electron emission γ_{Ti} from titanium and a proton current to the foil I^p . Data processing of five experiments provide:

$$\gamma_{Ti} = 1.7 \pm 0.1, \quad I^p \approx 1.85 \text{ A.}$$

Let coefficients of the secondary electron emission from the titanium foil surface for protons and neutrals are equal (at same values of kinetic energy), then from the balance equation one can estimate an equivalent current of neutrals $I^n \approx 0.7$ A. Thus, at the recuperator entrance the beam consists of neutrals by more than 30%. The operating vacuum in the installation is about 10^{-5} Torr. If we assume the charge-exchange cross-section equal to $2 \cdot 10^{-15} \text{ cm}^2$, for a drift chamber 1 m long the part of recharged ions is 6%. According to Ref. [5] for the Start-type sources the output beam consists of ions

Table 3

Comparison of Maximum Characteristics of Different Systems of Recuperator

Parameters	U_0 , kV	j_0 , mA/cm ²	I , mA	P , $\mu\text{A}/\text{B}^{3/2}$	W , kW	η , %
Flat collector	5.0	7.2	145	0.3	0.64	55
	10.6	200	3000	5.0	30	43
Cup without grid	5.0	4	80	0.2	0.40	73
	10.6	205	3500	5.2	32	48
Cup with grid	5.0	5	85	0.2	0.42	67
	10.6	200	3300	5.0	32	45
Flat collector [2]	100	0.7	30	$1 \cdot 10^{-3}$	2.7	77
Flat collector [3]	100	1.25	50	$1.6 \cdot 10^{-3}$	4.7	64

by 85% and by 15% of atoms, born in the course of a charge-exchange of a primary ion beam in the source-outflowing gas cloud. Taking into account the low efficiency of beam generation at $U_0=10$ kV (as the ion-optical system of the present source had been designed for $U_0 \simeq 25$ kV), a 25% charge-exchange of the beam seems quite possible.

CONCLUSION

In Table 3 there are given comparative characteristics for different systems of a recuperator; U_0 is the voltage of ion injection, I_{col} , U_{col} are the current and voltage of the collector, which correspond to the maximum recuperating power W . Two regimes: one with a maximum efficiency, the other with a maximum power value of the recuperated beam are given for each type of a recuperator. There are also presented results of experiments [3] with a flat recuperator, which design is similar to that studied in the present paper, but which geometric dimensions fit (for) a considerably smaller beam density. The results obtained permit the following conclusions to be made, that at high values of a beam power all the three types of the recuperator presented here have an approximately equal efficiency. For an intense beam ($P \sim 5 \mu\text{A}/\text{V}^{3/2}$) it is about 45%, for beams of lower intensity ($P \sim 0.2 \mu\text{A}/\text{V}^{3/2}$) the recuperator with a Faraday cup collector provides the highest efficiency of 70%.

The use of grids for plasma component separation results in a considerable decrease in the recuperator efficiency.

The authors gratefully acknowledge the support of I.N. Golovin, and G.I. Dimov and the fruitful discussions with

G.V. Roslyakov and V.I. Davidenko.

REFERENCES

1. Post R. B.E.N.S. Nuclear Fusion Reactor Conference. September, 1960, Paper 2.1, p.88.
2. Barr W.L., Moir R.W., Hamilton C.W., Lietzke A.F. Test of High Power Direct Conversion on Beams and Plasma.—Proc. 8th Symp. Eng. Problems of Fusion Research. 1979, v.2, p.1029—1033.
3. Barr W.L., Moir R.W. Test Results on Plasma Direct Converters.—Nuclear Tech./Fusion, 1983, v.3, N 1, p.98—111.
4. Kudelainen V.I., Meshkov I.N., Parkhomchuk V.V. et al. Depp Electron Beam

Deceleration in the System with the Longitudinal Magnetic Field.—J.T.P., 1976, v.46, N 8, p.1678.

5. Davidenko V.I., Dimov G.I., Morozov I.I., Roslyakov G.V. Multiampere Pulsed Proton Source.—Preprint INP 82-49, Novosibirsk, 1982.
6. Davidenko V.I. Formation of the High Perveance Ion and Atom Beams.—Doctorate Theses, INP, Novosibirsk, 1986.
7. Dimov G.I., Roslyakov G.V., Savchenko O.I. Formation of the Atom and Ion Beams from the Pulsed Plasma Arc-Discharge Source.—Preprint INP, Novosibirsk, 1967.
7. Physics Division. Atomic Data for Controlled Fusion Research. Febr., 1977, Oak Ridge, Tennessee.

*V.I. Guselnikov, I.N. Meshkov, T.I. Orishich
V.Ya. Savkin, V.P. Funtikov*

**Energy Recuperation
of Intense Proton Beam
Neutralized by Slow Electrons**

*В.И. Гусельников, И.Н. Мешков, Т.И. Оришич,
В.Я. Савкин, В.П. Фунтиков*

**Рекуперация энергии
интенсивного пучка протонов,
компенсированного медленными электронами**

Ответственный за выпуск С.Г.Попов

Работа поступила 5 августа 1988 г.
Подписано в печать 7.06 1989 г. МН 10248
Формат бумаги 60×90 1/16 Объем 1,5 печ.л., 1,2 уч.-изд.л.
Тираж 250 экз. Бесплатно. Заказ № 82

*Набрано в автоматизированной системе на базе фото-
наборного автомата ФА1000 и ЭВМ «Электроника» и
отпечатано на ротапринтере Института ядерной физики
СО АН СССР,
Новосибирск, 630090, пр. академика Лаврентьева, 11.*